

See discussions, stats, and author profiles for this publication at: <https://www.researchgate.net/publication/5603803>

Protein osmotic pressure modulates actin filament length distribution

ARTICLE *in* JOURNAL OF THEORETICAL BIOLOGY · MAY 2008

Impact Factor: 2.12 · DOI: 10.1016/j.jtbi.2007.12.012 · Source: PubMed

READS

14

2 AUTHORS, INCLUDING:



[Enrico Grazi](#)

University of Ferrara

171 PUBLICATIONS 1,550 CITATIONS

SEE PROFILE



This article was published in an Elsevier journal. The attached copy is furnished to the author for non-commercial research and education use, including for instruction at the author's institution, sharing with colleagues and providing to institution administration.

Other uses, including reproduction and distribution, or selling or licensing copies, or posting to personal, institutional or third party websites are prohibited.

In most cases authors are permitted to post their version of the article (e.g. in Word or Tex form) to their personal website or institutional repository. Authors requiring further information regarding Elsevier's archiving and manuscript policies are encouraged to visit:

<http://www.elsevier.com/copyright>



Protein osmotic pressure modulates actin filament length distribution

Enrico Grazi*, Sara Pozzati

Department of Biochemistry and Molecular Biology, Ferrara University, Via Borsari 46, 44100 Ferrara, Italy

Received 11 May 2007; received in revised form 3 July 2007; accepted 11 December 2007

Available online 27 December 2007

Abstract

1. The changes of the macromolecular osmotic pressure associated with F-actin solutions are related to the changes of the free energy of the free actin monomers.
2. By making use of the model of Biron et al. [2006. Inter-filament attractions narrow the length distribution of actin filaments. *Europhys. Lett.* 73, 464–470], the changes of the free energy of the free actin monomers are related to the changes of the length distribution of the actin filaments.

On these bases, we propose that the length distribution of the actin filaments is regulated by (a) the free energy of hydrolysis of ATP and (b) the macromolecular osmotic pressure.

- a. While the free energy of hydrolysis of ATP tends to zero, the length distribution of the actin filaments shifts from an exponential curve to a straight line parallel to the abscissa axis (i.e. the concentration of the actin filaments becomes independent of their length). In the mean time, the total energy of the actin filaments reaches a minimum.
- b. With the increase of the macromolecular osmotic pressure the free energy of the actin monomers increases and a break is introduced in the curve that describes the length distribution of the actin filaments; the break is located at the mean length of the filaments.

© 2007 Elsevier Ltd. All rights reserved.

Keywords: Actin; Filaments; Rearrangement; Water; Chemical; Potential

1. Introduction

At the steady state the length distribution of actin filaments is exponential (Kawamura and Maruyama, 1970), a distribution confirmed by many laboratories (Burlacu et al., 1992; Edelstein-Keshet and Ermentrout, 1998; Ermentrout and Edelstein-Keshet, 1998; Sept et al., 1999; Fujiwara et al., 2002; Biron and Moses, 2004). Furthermore, at moderate actin concentration, the exponential distribution is wide in the sense that its width (σ_1) is equal to its mean ($\langle l \rangle$). This is measured by the coefficient of variation, defined as $C_\sigma = (\sigma_1 / \langle l \rangle)$, which in the exponential case equals 1 (Biron and Moses, 2004). Furthermore, the length distribution is reported to display a mean of 7 μm (2600 actin monomers), the mean being

independent of the initial concentration of the actin monomer from 5 to 100 μM (Sept et al., 1999). This exponential distribution is grossly altered either by charge neutralization with multivalent cations (Strzelecka-Golaszewka et al., 1978; Grazi et al., 1982) or by the increase of protein osmotic pressure (Suzuki et al., 1989; Schwienbacher et al., 1995). These factors promote the conversion of the actin filaments into bundles of filaments. A smaller perturbation of the exponential length distribution of F-actin is also produced by the actin crosslinking protein, α -actinin, and by the capping proteins (Biron and Moses, 2004).

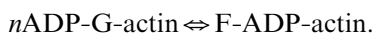
In this respect, the recent work of Biron et al. (2006) is of extreme relevance. These authors show that the exponential length distribution of F-actin dramatically narrows in the presence of: (i) crosslinker proteins, (ii) polyvalent counterions, or (iii) depletion mediated attractions. Furthermore the authors present a theoretical model which

*Corresponding author. Tel.: +39 0532 455421; fax: +39 0532 455419.
E-mail address: gre@unife.it (E. Grazi).

predicts that in equilibrium, short-range attractions enhance the tendency of filaments to align parallel to each other, eventually leading to an increase in the average filament length and a decrease in the relative width of the distribution of filament lengths. The same model allows to predict the length distribution of the actin filaments and to calculate their free energy.

In this work, we relate the protein osmotic pressure, associated with F-actin solutions, to the changes of the free energy of the free actin monomer (Appendix A) and, by making use of the model of [Biron et al. \(2006\)](#) (Appendix B), we further relate the change of the free energy of the free actin monomer to the changes of the length distribution of the actin filaments.

This is possible provided that the F-actin system is in equilibrium:



Under these circumstances all the actin filaments and the monomer display the same concentration. If now the osmotic equilibrium is perturbed by the addition of an external macromolecule, a new actin filament length distribution is produced, due to the onset of short-range attractions. Modelling of the new filament length distribution can be achieved provided that the corresponding value of the short-range attractions is known. This latter is the value of the short-range attractions, which makes the change of the free energy of the free actin monomer, calculated according to [Biron et al. \(2006\)](#), equal to that obtained from the osmotic experiments.

2. Materials and methods

Cellulose dialysis tubing (M , cutoff 6000) was purchased from Medicell International. Poly(ethyleneglycol) 40,000 was purchased from Serva Electrophoresis GmbH. G-actin was prepared from rabbit skeletal muscle according to [Spudich and Watt \(1971\)](#). Its molar concentrations were calculated on the basis of an M_r value of 42 kDa ([Collins and Elzinga, 1975](#)). The absorption coefficient used was $A_{290}^{1\%} = 6.2$ ([Gordon et al., 1976](#)).

The viscosity of F-actin solutions was measured with an Ostwald viscosimeter maintained at $21 \pm 0.1^\circ\text{C}$.

2.1. The dialysis of F-actin

F-actin solutions, 120–168 μM as the monomer, were dialyzed for 24 h at 2°C (first dialysis) against a buffer solution containing per 1000 g of water: KCl, 0.1 mol; triethanolamine, 0.01 mol; MgCl_2 , NaN_3 , 2-mercaptoethanol, 2 mmol each; ATP and CaCl_2 , 0.1 mmol each. pH was taken to be 7.45 with 6 N HCl (buffer A). The dialyzed actin solution was diluted with the same buffer to the concentration selected for the experiment, 12–48 μM . The resulting actin solution (10–12 mL) was dialyzed (second dialysis) overnight at 21°C against 2 L of buffer A. The dialysis tube was open at the upper extremity and care was

taken to maintain the inner and the outer solutions at the same level. At the end of the dialysis, the concentration and the viscosity of actin were determined. Specific viscosity of F-actin 19.2 μM was 0.8. The nonpolymerizable fraction of F-actin was never larger than 0.11 μM . This figure was obtained by centrifugation of 0.2 ml aliquots of the protein solution at 393,000g for 10 min at 21°C in the TL100 rotor of the Beckmann TL100 centrifuge and by assaying the supernatant solution for protein by the Coomassie Blue method ([Bradford, 1976](#)), as modified by [Stoscheck \(1990\)](#). To perform the experiment 1 mL aliquots of the actin solution were transferred by means of 1 mL Pedersen micropipette into dialysis bags. These were then dialyzed, with stirring, against 100 mL aliquots of buffer A taken from the same solution used for the second dialysis. Dialysis was performed at 21°C in stopped bottles (beside a small hole in the stop cock), immersed in a water-bath thermostatically controlled to within $\pm 0.1^\circ\text{C}$. Also in this case the dialysis bag was open at the upper extremity and care was taken to maintain the inner and the outer solutions at the same level. Dialysis was prolonged up to 12 days while the volume of the protein solution was controlled from time to time. At the end of the experiment the volume of the protein solutions was measured by means of Pedersen micropipettes and the viscosity was determined. Usually the 1 mL protein solution was fully recovered.

A possible concern is the time length of the experiments. We found that F-actin is stable provided that the solutions are supplemented with 2-mercaptoethanol. To check the stability of F-actin we selected viscosity. At the end of the experiments 80–100% of the original viscosity was recovered. Furthermore the same F-actin could be depolymerized and repolymerized successfully. Initially specific viscosity, η_{sp} , of F-actin 19.2 μM (10 mL) was 0.8. At the end the samples were combined, depolymerized against 5 mM triethanolamine-HCl, 2 mM 2-mercaptoethanol, 0.1 mM ATP and 0.1 mM CaCl_2 , diluted to 10 mL and repolymerized by the addition of 2 mM MgCl_2 . F-actin was 17 μM , η_{sp} was 0.66, the decrease was due mostly to mechanic losses.

2.2. The dialysis of F-actin against poly(ethylene glycol) 40,000 solutions

F-actin solutions were prepared as described in the section, *The dialysis of F-actin*, with the difference that at the time of the third dialysis to the 100 mL aliquots of buffer A, 0.03–1.6 g of poly(ethyleneglycol) 40,000 were added. Equilibration was then performed up to 9 days at 21°C . At the end of the experiment the volume of the protein solutions was measured by means of Pedersen micropipettes and the viscosity was determined. Usually 80–100% of the original viscosity was recovered. The addition of poly(ethyleneglycol) decreases the concentration of the small electrolytes up to 1.32% (the density of poly(ethyleneglycol) is 1.21 g/mL). It is very unlikely

however that these changes influence the results significantly.

2.3. The macromolecular osmotic pressure induced by poly(ethyleneglycol)

Osmotic pressure associated with poly(ethyleneglycol) solutions (up to 5 g per 100 g of water) was measured by means of osmometers equipped with UH 100125 Schleicher and Schuell membranes, M_r , cutoff 25,000. The macromolecular osmotic pressure generated by poly(ethyleneglycol) is related to the concentration of the macromolecule by

Macromolecular osmotic pressure

$$= 980(9c + c^{2.71}) \text{ dyne/cm}^2,$$

where c is the concentration of poly(ethyleneglycol) (weight per 100 ml of solution).

3. Results

3.1. Protein osmotic pressure associated with F-actin solutions of moderate concentrations

F-actin solutions (1 mL) 10–60 μM , as the monomer, were dialyzed against buffer A (see Materials and methods). It was expected that F-actin, a nondiffusible species, by decreasing the chemical potential of water, would generate an inward flux of water and a concomitant increase of the volume of the protein compartment. Dialysis was prolonged up to 288 h at 21 °C but the volume of the dialyzed solutions was essentially unchanged (1 ± 0.005 mL). The change of the water chemical potential induced by F-actin was thus undetectable.

3.2. Equilibration of F-actin solutions against poly(ethylene glycol) 40,000 solutions

F-actin solutions were also equilibrated against poly(ethyleneglycol) solutions of increasing concentration. In this case, under the effect of poly(ethyleneglycol), the volume of the actin solution decreased significantly as a function of the increase of the concentration of poly(ethyleneglycol). The final actin concentration was calculated by the formula:

$$\text{Final concentration} = \frac{\text{initial volume} \times \text{initial concentration}}{\text{final volume}}.$$

The results of these experiments are shown in Fig. 1 where the macromolecular osmotic pressure (P) at the equilibrium is plotted against the actin concentration.

In the first series of experiments (filled circles) the starting concentration of actin was 19.2 μM , as the monomer. This sample was equilibrated against buffer A without poly(ethyleneglycol). After 168 h of equilibration at 21 °C the volume of the sample, thus the concentration of actin, was unchanged (1 ± 0.005 mL). The other samples were equilibrated for the same time in the presence of

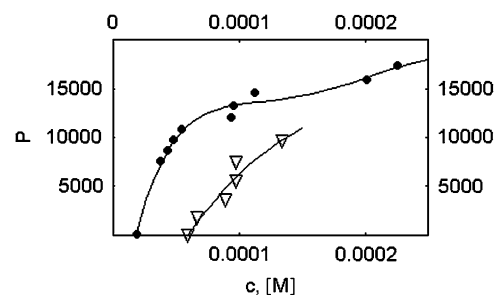


Fig. 1. Macromolecular osmotic pressure (dyne/cm²) as a function of total actin concentration. Filled circles: initial actin concentration 19.18 μM ; open triangles: initial actin concentration 60 μM .

increasing concentrations of poly(ethyleneglycol). At the end of the experiments their volume was measured and the actin concentration was calculated. The relationship between total actin concentration, c , and the macromolecular osmotic pressure is given by

$$\begin{aligned} \text{Macromolecular osmotic pressure} = & -17506.66 \\ & + 1.876 \times 10^9 c - 2.7338 \times 10^{11} c^{1.5} + 1.2539 \times 10^{13} c^2 \\ & - 8.7418 \times 10^{15} c^3 \text{ dynes/cm}^2. \end{aligned} \quad (1)$$

The equation is only aimed at describing the data and is valid only in their range.

In the second series of experiments (open triangles) the starting concentration of F-actin was 60 μM , as the monomer. This sample was equilibrated against buffer A without poly(ethyleneglycol). After 173 h of equilibration at 21 °C its volume was unchanged (1 ± 0.005 mL). The other samples were equilibrated for the same time in the presence of increasing concentrations of poly(ethyleneglycol). At the end of the experiments their volume was measured and the actin concentration was calculated.

The relationship between total actin concentration, c , and the macromolecular osmotic pressure is given by

$$\begin{aligned} \text{Macromolecular osmotic pressure} = & -13761 \\ & + 2.8393 \times 10^8 c - 9.3939 \times 10^{11} c^2 + 9.544 c^3 \\ & + 7.8378 \times 10^{11} c^4 \text{ dynes/cm}^2. \end{aligned} \quad (2)$$

The equation is only aimed at describing the data and is valid only in their range.

The results of Fig. 1 show the divergent properties of resting and perturbed F-actin solutions. A resting solution of 60 μM actin does not develop a detectable osmotic pressure and the water chemical potential of the solution is essentially that of buffer A. On the contrary the actin solution concentrated from 19.18 to 54.86 μM develops a macromolecular osmotic pressure of 10,852 dyne/cm², i.e. the change of the water chemical potential is

$$\begin{aligned} \Delta\mu_w = -PV_M = & -10852 \times 18 = -195336 \text{ erg/mol of water,} \\ \text{or} & -7.877 \times 10^{-6} \text{ RT/mol of water.} \end{aligned}$$

$\Delta\mu_w$ is the change of the water chemical potential, V_M the partial molar volume of water, 18 cm³. The water chemical

potential of the actin solution is by 7.877×10^{-6} RT/mol of water lower than the water chemical potential of buffer A.

Thus two F-actin solutions of identical concentration display a different physical-chemical behavior. This is easily explained provided that the actin filament length distribution is different in the two cases.

3.3. The macromolecular osmotic pressure and the free energy of the actin monomer

This is indeed the case since the free energy of the actin monomer changes as a function of the macromolecular osmotic pressure associated with the actin solution. As it is illustrated in Appendix A, the free energy change of the free actin monomer can be calculated by integration of equation, Eq. (A.7)

$$d\mu_1 = (w/m)V_M(dP/dm) dm,$$

where $\Delta\mu_1$ is the change of the chemical potential of the free actin monomer, P is the protein osmotic pressure, w is the number of moles of water, m is the number of moles of the actin monomer (free and embedded into the polymers) and V_M is the water partial molar volume. The integration is performed after substitution of the term P either with Eq. (1) or with Eq. (2) which relates the macromolecular osmotic pressure to the total concentration of actin. The result of this procedure is presented in Fig. 2 that describes the increase of the free energy per mol of free actin monomer as a function of total actin concentration. In the first experiment (filled circle) the increase of total actin concentration from 19.18 to 48 μM and to 226 μM increases the free energy of the free actin monomer by 13.36 and by 16.77 RT/mol of free monomer, respectively. In the second experiment the increase of the total actin concentration from 60 to 98.18 μM and to 135 μM increases the free energy of the free actin monomer by 3.13 and by 4.5 RT/mol of free monomer, respectively.

3.4. Calculating the actin filament length distribution at the steady state

According to Sept et al. (1999), the mean of the length distribution of the actin filaments is $\sim 7 \mu\text{m}$ and it is

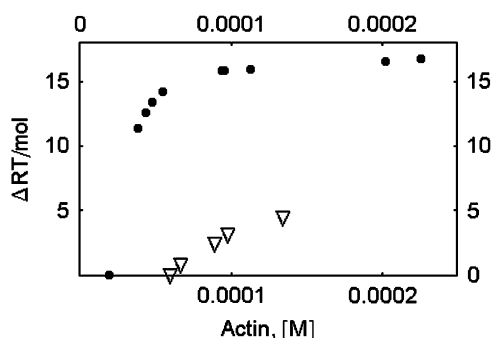


Fig. 2. The change of the free energy of the free actin monomer as a function of the total actin concentration. Filled circles: initial actin concentration 19.18 μM ; open triangles: initial actin concentration 60 μM .

independent of the total actin mass between 0 and 100 μM actin, as the monomer. The model of Biron et al. (2006) offers the opportunity to reproduce the distribution observed by Sept et al. (1999) by making use of Eq. (B.2) (Appendix B). The operation is done by setting the average numerical length, l^* , to $2560 = 7000 \text{ nm}/2.73 \text{ nm}$, where 2.73 nm is the length increment per actin subunit (Hanson and Lowy, 1963) by setting the maximum numerical length of the filaments to 25,600 (69,888 nm) and by setting the short-range attraction per monomer, u_0 , to the very low value of $-10^{-15} k_B T$ in order to minimize the short-range attractions and to obtain an exponential curve (Appendix B). In Fig. 3, the distribution found by Sept et al. (1999) is reproduced for two F-actin concentrations, 19.18 and 110 μM , as the monomer. The two distributions display the same average length of the filaments, 7 μm . However, the concentration of the free monomer differs in the two cases, being 2.923 and 16.744 pM at 19.18 and 110 μM total monomer, respectively.

3.5. The filament distribution associated with the free energy minimum of the actin filaments

The total free energy of the actin filaments, displaying the length distribution shown in Fig. 3, is calculated by making use of Eqs. (B.3) and (B.4) (Appendix B). At 19.18 μM total actin the total free energy of the filaments is 7.495×10^{-9} RT per liter of solution and at 110 μM total actin the total free energy of the filaments is 4.29×10^{-8} RT per liter of solution. These, however, are not the minimum free energy level of the filaments. In fact a further decrease of the free energy of the actin filaments occurs with the increase in their average filament length. The free energy minima are attained at the average filament length of 34,944 nm (12,800 monomers) and are, 1.5×10^{-9} RT per liter of solution at 19.18 μM total actin and 8.594×10^{-9} RT per liter of solution at 110 μM total actin. At the free energy minimum all the actin filaments,

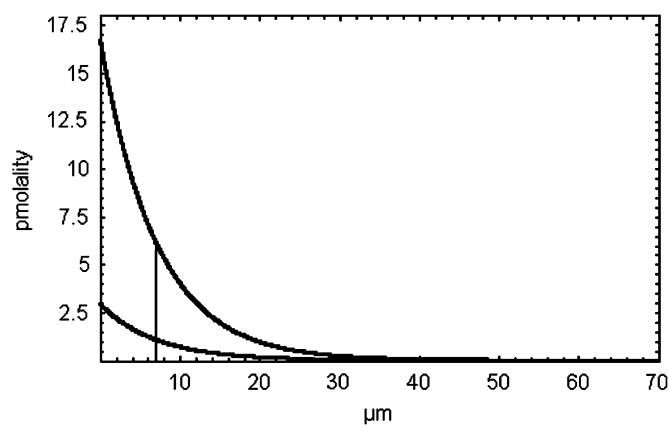
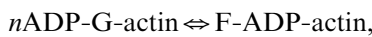


Fig. 3. Distribution of the actin filaments in F-actin solutions at the steady state. Upper line: total monomer concentration, 110 μM ; free monomer concentration, 1.6744×10^{-11} M; lower line: total monomer concentration, 19.18 μM ; free monomer concentration, 2.923×10^{-12} M; the vertical line indicates the average filament length, 7 μm .

monomer included, display the same concentration, 0.0586 and 0.3357 μM at 19.18 and at 110 μM total actin, respectively (Fig. 4).

The question now is why at the filament distribution described by Sept et al. (1999) are the actin filaments not at the free energy minimum. The answer is that, under the usual conditions, the polymerization of actin is coupled to the hydrolysis of ATP. Thus the system is not at the true equilibrium. When all the ATP of the solution has been hydrolyzed the polymerization of actin is simply described by the reaction,

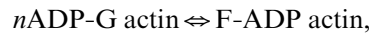


the actin filaments are allowed to reach their free energy minimum and their distribution is characterized by all the filament concentrations being equal.

3.6. The effect of the dialysis against poly(ethyleneglycol) on the length distribution of the actin filaments

We have shown that resting actin solutions display an osmotic behavior different from that of the actin solutions of comparable concentration but perturbed by the dialysis against poly(ethyleneglycol). We explain this feature with a rearrangement of the distribution of the actin filaments, so that, as an example, the distribution of the actin filament of a 60 μM resting actin solution is different from that of a 60 μM actin solution obtained by the concentration of an originally 19.18 μM actin solution. To demonstrate the perturbing effect of the dialysis against poly(ethyleneglycol) we take as the starting point the equilibrium distribution of the actin filaments (Fig. 4). In our experiments, owing to the long times of dialysis and the associated hydrolysis of ATP, it is likely that, in the

absence of poly(ethyleneglycol), the system evolves toward the condition,



thus toward the equilibrium. On the contrary, in the presence of poly(ethyleneglycol), the system shifts to a new filament length distribution prompted by the onset of short-range attractions. These attractions are simulated by decreasing the value of u_0 (the short-range attraction per monomer) until the change of the free energy of the free actin monomer, calculated according to Biron et al. (2006), matches that obtained in the osmotic experiments. Once this is made the distribution of the actin filaments is calculated. The results of the calculations are presented in Table 1 where the properties of the resting F-actin solutions are compared with the properties of the perturbed F-actin solutions of the same concentration, which are obtained by dialysis against poly(ethyleneglycol), starting from actin solutions of lower concentration. As shown in Table 1, the concentration of the free actin monomer of the perturbed F-actin solutions is very slightly decreased, and C_σ is slightly decreased compared to that of the resting F-actin solutions. The ratio, free energy/free actin monomer, increases from $\sim 10^{-8} k_B T$ (resting solutions) to $14.215 k_B T$ (perturbed solutions). Concomitantly u_0 (the short-range attraction per monomer) decreases from $-10^{-15} k_B T$ (resting solutions) to $-5.33 \times 10^{-7} k_B T$ (perturbed solutions). Surprisingly u_0 reaches its lowest value, $-5.33 \times 10^{-7} k_B T$, at 54.86 μM total perturbed actin while it increases at larger total actin concentrations, being, $-3 \times 10^{-7} k_B T$, at 213.44 μM total perturbed actin. It is unreasonable that short-range attractions decrease with the increase of the concentration; it is thus likely that one or more influent parameters escaped recognition in the model.

The effects of the change of u_0 on the distribution of the actin filament is presented in Fig. 5 where the behavior of a 19.18 μM actin solution concentrated, by dialysis against different concentrations of poly(ethyleneglycol), to 38.4 μM (upper figure), 54.84 μM (middle figure) and 93.66 μM (lower figure). As shown in the figure, the concentration of the actin filaments increases with their length while, at equilibrium (Fig. 4), the concentration is independent of the length. Furthermore, all the curves display a break at the mean length.

4. Discussion

Merging the model of Biron et al. (2006) that relates the free energy of the actin filaments to their length distribution and our studies that relate the free energy of the free actin monomer to the water chemical potential, we define three conditions for the F-actin solutions

- the steady state where the concentration of the actin filaments is exponentially related to their length (Fig. 3);

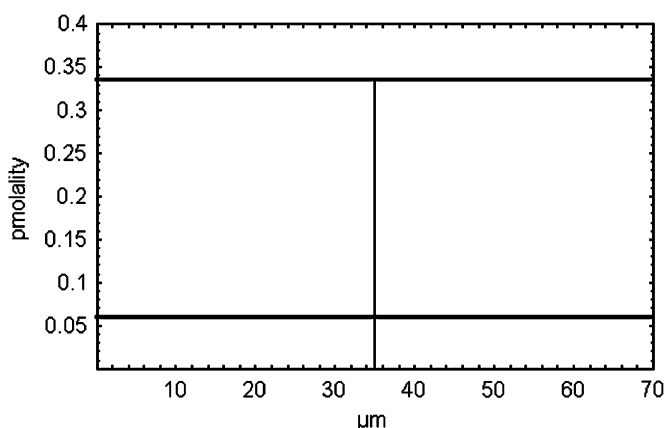


Fig. 4. Distribution of the actin filaments in F-actin solutions at the equilibrium. Upper line: total monomer concentration, 110 μM ; free monomer concentration, $3.357 \times 10^{-13} \text{ M}$; lower line: total monomer concentration, 19.18 μM ; free monomer concentration, $5.8638 \times 10^{-14} \text{ M}$; the vertical line indicates the average filament length, 34.94 μm . The value of $C_\sigma = 0.557328$ and of $u_0 = -10^{-15} k_B T$ is the same for the two samples; the value of a equals $1.4195 \times 10^{-30} k_B T$ for 19.18 μM actin and $8.1269 \times 10^{-30} k_B T$ for 110 μM actin.

Table 1
Comparison of the properties of resting F-actin solutions with the properties of perturbed F-actin solutions concentrated by dialysis against poly(ethyleneglycol)

Total actin monomers (μM)	Free actin monomers (pM)	C_σ	u_0	$k_B T/\text{mon.}$
Resting F-actin solutions				
38.4	0.113774	0.577328	-10^{-15}	2.80×10^{-8}
54.86	0.162581	0.577328	-10^{-15}	2.70×10^{-8}
93.66	0.277516	0.577328	-10^{-15}	3.56×10^{-8}
Perturbed F-actin solutions				
38.4	0.11371	0.577302	-5.10×10^{-7}	11.378
54.86	0.16258	0.577287	-5.33×10^{-7}	14.215
93.66	0.277452	0.577278	-4.51×10^{-7}	15.778
213.44	0.669419	0.577271	-3.10×10^{-7}	16.77

The original concentration of the perturbed F-actin solutions, concentrated by dialysis against poly(ethyleneglycol) was $19.18 \mu\text{M}$. The concentrations indicated in the Table were reached after equilibration with poly(ethyleneglycol) solutions generating the macromolecular osmotic pressure of 7535, 10852, 13281, 17305 dyne/cm², respectively.

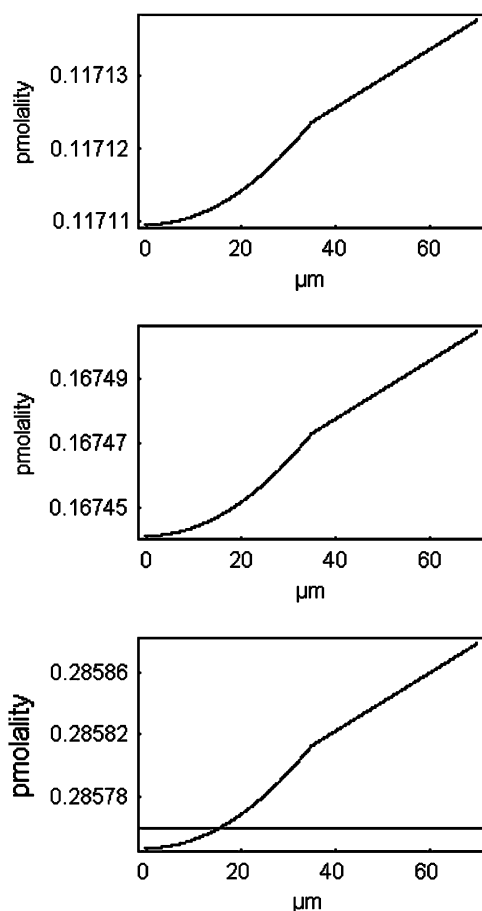
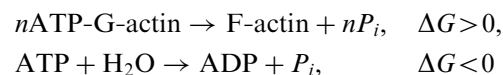


Fig. 5. Proposed actin filament length distribution in F-actin solutions equilibrated against poly(ethyleneglycol)—Abscissa, filament length, μm ; ordinate, filament concentration, pM. Initial F-actin concentration, $19.18 \mu\text{M}$, as the monomer. Final F-actin concentration: upper figure, $38.4 \mu\text{M}$; middle figure, $54.86 \mu\text{M}$; lower figure, $93.66 \mu\text{M}$. The break coincides with the mean length of the actin filament, $34.94 \mu\text{m}$. The maximum filament length is $69.89 \mu\text{m}$.

(b) the equilibrium where the concentration of the actin filaments is independent of their length (Fig. 4);

(c) the equilibrium perturbed by an external macromolecule where the concentration of the actin filaments increases very slightly as a function of their length, with a break at the mean length.

So, in addition to the contribution of either capping or gelling or severing proteins, we propose that the length distribution of the actin filaments is ruled by the coupling of the polymerization reaction with the reaction of hydrolysis of ATP,



and by the osmotic stress generated by the surrounding macromolecules.

Concerning the first point we predict that, while the free energy of hydrolysis of ATP approaches zero, the total free energy of the actin filaments decreases and their average length increases, so that, at the equilibrium, the total free energy of the actin filaments reaches a minimum and the concentration of the actin filaments becomes independent of their length. Sept et al. (1999) showed that the mean length of the actin filaments is $\sim 7 \mu\text{m}$ while Kaufmann et al. (1982) and Käs et al. (1996) found a mean length of $22 \mu\text{m}$. According to our hypothesis the two mean lengths should be associated with different free energies of the reaction of hydrolysis of ATP, the steady state in the experiment of Sept et al. (1999) being farther from the equilibrium. We predict also that the free energy of the free actin monomer as well as the length distribution of the actin filaments are dictated by the macromolecular osmotic stress, not only for a system in equilibrium, as we have made for simplicity in our example, but also at any steady state. The increase of the macromolecular osmotic stress is expected to increase the free energy of the free actin monomer and to introduce a break in the curve that describes the concentration of the actin filaments as a function of their length.

Cells move because of the cyclic sequence of anterior membrane protrusion, contact with the underlying substrate and retraction of the posterior trailing edge. The most active region is the leading lamellipodium, an area very rich in actin filaments in the form of dense webs and small bundles. The assembly and the disassembly of the actin filament is a very complex phenomenon, regulated at many levels. To the process contribute many ancillary proteins with different functions: the capping, the gelling, the severing, the cross-linking proteins, the Arp2/3 complex. A further level of regulation is provided, as an example, by the Rho family GTPase *rac1*, the inhibition of *rac1* and to a lesser extent of *cdc42* and RhoA blocks motility at the cell periphery (Wittmann et al., 2003; Noritake et al., 2004). Additional, basic mechanisms of regulation are macromolecular crowding and ATP concentration. Macromolecular crowding is important *per se* and because it modulates the properties of the ancillary cytoskeleton proteins. At a suitable level it promotes the conversion of the actin filaments into actin bundles. The level is enhanced in the presence of tropomyosin and is decreased in the presence of either caldesmon or filamin (Cuneo et al., 1992). Macromolecular crowding orients the gelling action of α -actinin mostly toward the actin bundles (Grazi et al., 1992) and hinders, because of the formation of actin bundles, the severing action of gelsolin (Grazi et al., 1991). ATP also is a potential tool of regulation. Due to the nonuniform distribution of ATP-generating and ATP-consuming systems a nonuniform ATP supply occurs in liver cells where proteins at the cell periphery, i.e. with a greater average distance from mitochondria, experience a more dramatic decrease in ATP concentration than protein in close proximity to mitochondria (Aw and Jones, 1985). Waves of ATP concentration propagate in the unidirectionally migrating plasmodium of *Physarum polycephalum*. ATP concentration is high at the frontal region and undulates over the whole plasmodium. In the mean time the typical birifrangent fibrils, composed of actin, myosin together with modulating proteins, are abundant where ATP concentration decreases (Ueda et al., 1990). ATP depletion causes the reversible disorganization of stress fibers in cultured vascular smooth muscle cells (Kwon et al., 2002). It thus appears that the concentration of ATP influences the behavior of actin in the cell; however, due to the multiplicity and the interaction of the regulation factors, it is uncertain whether *in vivo* the changes of the ATP concentration will display the same effects as *in vitro*.

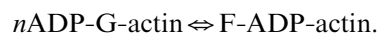
Acknowledgment

This work was supported by grants of the Università di Ferrara and of the Cassa di Risparmio di Ferrara.

Appendix A

A.1. The relationship between the chemical potential of water and the chemical potential of the free actin monomer in F-actin solutions

In our experiments because of the low initial concentration of ATP, 0.1 mM, of the long time of incubation and the treadmilling of the actin filaments, which leads to the hydrolysis of ATP, the polymerization can be described as a true equilibrium process:



Thus, according to the Gibbs–Duhem relationship, we write

$$-w d\mu_w = a_1 d\mu_1 + a_2 d\mu_2 + a_3 d\mu_3 + \dots + a_n d\mu_n, \quad (\text{A.1})$$

where w is the number of mol of water, a_1 is the number of mol of the actin monomer, a_2 – a_n are the number of mol of the actin polymers and the $d\mu$ are the chemical potential differentials of the single species.

Since the system is at the equilibrium, we also write

$$\begin{aligned} 2\mu_1 &= \mu_2, \\ \mu_1 + \mu_2 &= \mu_3, \\ \dots \\ \mu_1 + \mu_{(n-1)} &= \mu_n. \end{aligned}$$

The expression holds if we write

$$\begin{aligned} 2\mu_1 + 2d\mu_1 &= \mu_2 + d\mu_2, \\ \mu_1 + d\mu_1 + \mu_2 + d\mu_2 &= \mu_3 + d\mu_3, \\ \dots \\ \mu_1 + d\mu_1 + \mu_{(n-1)} + d\mu_{(n-1)} &= \mu_n + d\mu_n. \end{aligned}$$

We also write

$$\begin{aligned} 2d\mu_1 &= d\mu_2, \\ d\mu_1 + d\mu_2 &= d\mu_3, \\ \dots \\ d\mu_1 + d\mu_{(n-1)} &= d\mu_n. \end{aligned}$$

Hence, Eq. (A.1) becomes

$$-w d\mu_w = d\mu_1(a_1 + 2a_2 + 3a_3 + \dots + na_n). \quad (\text{A.2})$$

We observe now that

$$m = a_1 + 2a_2 + 3a_3 + \dots + na_n \quad (\text{A.3})$$

is the total concentration of the monomers, free plus embedded in the polymers and by substituting the expression in Eq. (A.2) we obtain

$$-w d\mu_w = m d\mu_1. \quad (\text{A.4})$$

This means that from the change of the water chemical potential we can calculate the change of the chemical potential of the free monomer in the system. Since

$$\mu_w = \mu_w^0 + RT \ln[a_w] \quad \text{and} \quad PV_M = RT \ln[a_w],$$

where a_w is the water activity, V_M is the water partial molar volume and P is the macromolecular osmotic pressure, we write

$$d\mu_w = -V_M dP, \quad (\text{A.5})$$

where V_M is the water partial molar volume and P is the macromolecular osmotic pressure; by introducing this expression in Eq. (A.4), we obtain

$$d\mu_1 = (w/m)V_M dP. \quad (\text{A.6})$$

Integration of the expression (A.6) under the form:

$$d\mu_1 = (w/m)V_M (dP/dm) dm \quad (\text{A.7})$$

yields $\Delta\mu_1$.

Appendix B

B.1. Calculating the distribution and the energy of the actin filaments in the F-actin solution

Biron et al. (2006) presented a theoretical model which shows that in equilibrium, short-range attractions enhance the tendency of filaments to align parallel to each other, eventually leading to an increase in the average filament length and a decrease in the relative width of the distribution. The same model allows to calculate the free energy (per unit volume) of the solution containing the actin filaments. For clarity we summarize the pertinent points of this work.

B.1.1. Nomenclature

$a = \alpha - \mu$; α , energy of interaction of neighboring monomers, independent of the length of the filament; b , end cap energy of the filaments; $C_\sigma = \sigma_1 / \langle l \rangle$, coefficient of variation; d , diameter of the actin filament; δ , is the range of the interaction potential and is obtained by multiplying the numerical average interfilament distance by $k_B T$; $g = \pi u_0^2$; l , numerical length of the filament; l^* , numerical length of the filament of average length; $l_1 \equiv \min(l, l')$; $l_2 \equiv \max(l, l')$; $\langle l \rangle_0$ = average length of the filaments; μ , free energy of the monomer; $\rho_0 = \exp[-b/v_0]$; ρ_1 = concentration of the free actin monomer; ρ_l , numerical concentration of the filament, l , in a distribution characterized by short-range interactions; $\rho_l^{(0)}$, numerical concentration of the filament in the absence of interactions; ρ^* , numerical concentration of the filament of average length; ρ_m , total monomer concentration; σ_1 , width of the distribution; $u_0 < 0$, short-range attraction per monomer; v_0 , volume of the monomer; $z \equiv (l_1/d) u_0$.

B.1.2. The distribution of the actin filaments

In the absence of interactions the distribution is exponential,

$$\rho_l^{(0)} = \rho_0 \exp[-al] \quad (\text{B.1})$$

with an average filament length, $\langle l \rangle_0 = 1/a = (\rho_m/\rho_0)^{1/2}$ and $C_\sigma = 1$.

In the presence of short-range attractions the distribution is described by the two expressions

$$\begin{aligned} \rho_l &= \rho_0 \exp[-al + (gl^* \rho^*) l^2] & \text{when } l \leq l^*, \\ \rho_l &= \rho_0 \exp[-(a - gl^{*2} \rho^*) l] & \text{when } l \geq l^*. \end{aligned} \quad (\text{B.2})$$

With three unknowns a, l^*, ρ^* , the distribution function, ρ_l , can be calculated by solving the following three equations:

- (i) the monomer conservation condition, $\int dl \rho_l = \rho_m$,
- (ii) The consistency condition,

$$\rho^* = \rho_0 \exp(-al^* + gl^{*3} \rho^*) \quad (\text{B.3})$$

- (iii) the condition that $\langle l \rangle = l^*$.

The free energy of the filaments in an F-actin solution

$$\begin{aligned} f &= \sum_l \rho_l (\ln[\rho_l v_0] - 1 + \alpha l + b) + \sum_{l < l'} w(l, l') \rho_l \rho_{l'} \\ &\quad - \mu \sum_l l \rho_l. \end{aligned} \quad (\text{B.4})$$

The logarithmic term represents the translational entropy of the filaments where v_0 is the monomer volume. Here and in the following, all energies are in units of the thermal energy $k_B T$. The energy of a single filament consists of a term linear in l which is due to the interaction between neighboring monomers and an l -independent term that is basically the end-cap energy, b , of the filaments. The next term introduces the short-range attractions and finally, the Lagrange multiplier μ is added to free energy to fix the total monomer concentration.

The short-range attractions, $w_{att}(l, l')$, are expressed by

$$\begin{aligned} w_{att}(l, l') &= \pi l' \delta (1 - \exp[-u_0]) / 2 \\ &\quad + 2\pi d \delta \{ 2l_1 (1 + (\exp[-z] - 1)/z) \\ &\quad + (l_2 - l_1) (1 - \exp[-z]) \}. \end{aligned} \quad (\text{B.5})$$

The first term is the contribution from configurations where the filaments cross at large angles while the second term is the contribution from parallel configurations with $z \equiv (l_1/d) u_0$, $l_1 \equiv \min(l, l')$ and $l_2 \equiv \max(l, l')$. The latter is divided into a term independent of l_2 due to configurations where the two rods overlap only partially and configurations where the short filament is fully adjacent to the long filament.

B.2. Operative features

B.2.1. Generalities

In their work Biron et al. (2006) use numerical length, numerical concentration and express free energy (per unit volume) in $k_B T$. We use the same units and, to avoid overflow in the calculation, the volume of reference is the μm^3 . When presenting the data the numerical length is

converted into length by multiplying by 2.73 nm (the length per actin filament subunit) (Hanson and Lowy, 1963), the concentration is converted from molecules/ μm^3 into mol/L and the free energy is expressed in RT/mol.

The maximum length of the actin filaments is set to 25,600 monomers, 69,888 nm.

The diameter of the actin filament, d , is set to 3.47895. This figure is obtained by dividing the diameter of the actin filament, 9.5 nm (Holmes et al., 1990) by 2.73 nm. The figure of 9.5 nm seems reasonable owing to the very low macromolecular osmotic pressure of our samples (Grazi, 1997).

The average inter-filament distance, δ , is calculated according to Oda et al. (1998): (number concentration of the filaments \times average length/ k)^{0.5}. The value of $k = 3.48943 \times 10^8$ is referred to a concentration expressed in μm^3 and is obtained from Fujime and Ishiwata (1971).

The volume of the actin monomer, $v_0 = 4.369 \times 10^{-8}/\mu\text{m}^3$, is taken from the partial specific volume of F-actin, 0.63–0.66 cm^3/g (Suzuki et al., 1996).

B.2.2. The distribution of the actin filaments in “resting” F-actin solutions

To calculate the distribution of the actin filaments in a “resting” solution of F-actin, the expression for the concentration of the free actin monomer is first derived from the upper part of Eq. (B.2),

$$\rho_1 = \rho_0 \exp[-al + (gl^*\rho^*)l^2] \quad (\text{B.6})$$

From this the expression for a is obtained

$$a = (gl^*\rho^* - \ln[\rho_1/\rho_0]) \quad (\text{B.7})$$

which is substituted for, a , into Eq. (B.3), to give

$$\rho^* = \rho_0 \exp[-(gl^*\rho^* - \ln[\rho_1/\rho_0])l^* + gl^{*3}\rho^*]. \quad (\text{B.8})$$

The value of the ratio ρ_1/ρ_0 is then selected which makes $C_\sigma = 1$. Furthermore, to minimize the short-range attractions, u_0 is set to $-10^{-15} k_B T$ and, according to Sept et al. (1999), l^* is set to 7 μm . At this point Eq. (B.8), is solved for ρ^* , with increasing values of ρ_1 , until the value of ρ_1 , is found which satisfies the value of the total concentration of the actin monomers ρ_m .

B.2.3. The free energy of the actin filaments in “resting” F-actin solutions

The free energy of the actin filaments in “resting” F-actin solutions is calculated by Eq. (B.4). In fact, for $u_0 = -10^{-15}$, the short-range attractions are very minor and Eq. (B.4) reduces to

$$f = \sum_l \rho_l (\ln[\rho_l v_0] - 1 + al + b) - \mu \sum_l l \rho_l \quad (\text{B.9})$$

and by taking into account that, $a = \alpha - \mu$, to

$$f = \sum_l \rho_l (\ln[\rho_l v_0] - 1 + al + b). \quad (\text{B.10})$$

References

- Aw, T.Y., Jones, D.P., 1985. ATP concentration gradients in cytosol of liver cells during hypoxia. *Am. J. Physiol. Cell Physiol.* 249, C385–C392.
- Biron, D., Moses, E., 2004. The effect of α -actinin on the length distribution of F-actin. *Biophys. J.* 86, 3284–3290.
- Biron, D., Moses, E., Borukhov, I., Safran, S.A., 2006. Inter-filament attractions narrow the length distribution of actin filaments. *Europhys. Lett.* 73, 464–470.
- Bradford, M.M., 1976. A rapid and sensitive method for the quantitation of microgram quantities of protein utilizing the principle of protein-dye binding. *Anal. Biochem.* 72, 248–254.
- Burlacu, S., Janmey, P.A., Borejdo, J., 1992. Distribution of actin filament lengths measured by fluorescence microscopy. *Am. J. Physiol.* 262, C569–C577.
- Collins, J.H., Elzinga, M., 1975. The primary structure of actin from rabbit skeletal muscle. Completion and analysis of the amino acid sequence. *J. Biol. Chem.* 250, 5915–5920.
- Cuneo, P., Magri, E., Verzola, A., Grazi, E., 1992. ‘Macromolecular crowding’ is a primary factor in the organization of the cytoskeleton. *Biochem. J.* 281, 507–512.
- Edelstein-Keshet, L., Ermentrout, B.G., 1998. Models for the length distributions of actin filaments: I. Simple polymerization and fragmentation. *Bull. Math. Biol.* 60, 449–475.
- Ermentrout, B.G., Edelstein-Keshet, L., 1998. Models for the length distributions of actin filaments: II. Polymerization and fragmentation by gelsolin acting together. *Bull. Math. Biol.* 60, 477–503.
- Fujime, S., Ishiwata, S., 1971. Dynamic study of F-actin by quasielastic scattering of laser light. *J. Mol. Biol.* 62, 251–256.
- Fujiwara, S., Takahashi, H., Tadakuma, T., Funatsu, S., Ishiwata, S., 2002. Microscopic analysis of polymerization dynamics with individual actin filaments. *Nat. New Biol.* 4, 666–673.
- Gordon, D.J., Yang, Y.Z., Korn, E.D., 1976. Polymerization of Acanthamoeba actin. Kinetics, thermodynamics, and co-polymerization with muscle actin. *J. Biol. Chem.* 251, 7474–7479.
- Grazi, E., 1997. What is the diameter of the actin filament? *FEBS Lett.* 405, 249–252.
- Grazi, E., Magri, E., Pasquali-Ronchetti, I., 1982. Multiple supramolecular structures formed by interaction of actin with protamine. *Biochem. J.* 205, 31–37.
- Grazi, E., Magri, E., Cuneo, P., Cataldi, A., 1991. The control of cellular motility and the role of gelsolin. *FEBS Lett.* 295, 163–166.
- Grazi, E., Cuneo, P., Magri, E., Schwenbacher, C., 1992. Preferential binding of alpha-actinin to actin bundles. *FEBS Lett.* 314, 348–350.
- Hanson, J., Lowy, J., 1963. The structure of F-actin filaments isolated from muscle. *J. Mol. Biol.* 6, 46–60.
- Holmes, K.C., Popp, D., Gebhard, W., Kabsch, W., 1990. Atomic model of the actin filament. *Nature* 347, 44–49.
- Käs, J., Strey, H., Tang, J.X., Finger, D., Ezzell, R., Sackmann, E., Janmey, P.A., 1996. F-actin, a model polymer for semiflexible chains in dilute, semidilute, and liquid crystalline solutions. *Biophys. J.* 70, 609–625.
- Kaufmann, S., Käs, J., Goldmann, W.H.E., Sackmann, E., Isenberg, G., 1982. Talin anchors and nucleates actin filaments at lipid membranes. A direct demonstration. *FEBS Lett.* 314, 203–205.
- Kawamura, M., Maruyama, K., 1970. Electron microscopic particle length of F-actin polymerized in vitro. *J. Biochem.* 67, 437–457.
- Kwon, O., Phillips, C.L., Molitoris, B.A., 2002. Ischemia induces alterations in actin filaments in renal vascular smooth muscle cells. *Am. J. Physiol. Renal Physiol.* 282, F1012–F1019.
- Noritake, J., Fukata, M., Sato, K., Nakagawa, M., Watanabe, T., Izumi, N., Wang, S., Fukata, Y., Kaibuchi, K., 2004. Positive role of IQGAP1, an effector of Rac1, in Actin-meshwork formation at sites of cell–cell contact. *Mol. Biol. Cell* 15, 1065–1076.
- Oda, T., Makino, K., Yamashita, I., Namba, K., Mae'da, Y., 1998. Effect of the length and effective diameter of F-actin on the filament

- orientation in liquid crystalline sols measured by X-ray fiber diffraction. *Biophys. J.* 95, 2672–2681.
- Schwienbacher, C., Magri, E., Trombetta, G., Grazi, E., 1995. Osmotic properties of the calcium-regulated actin filament. *Biochemistry* 34, 1090–1095.
- Sept, D., Xu, J., Pollard, T.D., McCammon, J.A., 1999. Annealing accounts for the length of actin filaments formed by spontaneous polymerization. *Biophys. J.* 77, 2911–2919.
- Spudich, J.A., Watt, S.J., 1971. The regulation of rabbit skeletal muscle contraction. I. Biochemical studies of the interaction of the tropomyosin–troponin complex with actin and the proteolytic fragments of myosin. *J. Biol. Chem.* 246, 4866–4871.
- Stoscheck, C.M., 1990. Increased uniformity in the response of the Coomassie blue G protein assay to different proteins. *Anal. Biochem.* 184, 111–116.
- Strzelecka-Golaszewka, H., Prochmiewicz, E., Drabikowski, W., 1978. Interaction of actin with divalent cations. Characterization of protein-metal complexes. *Eur. J. Biochem.* 88, 219–227.
- Suzuki, A., Yamazaki, M., Ito, T., 1989. Osmoelastic coupling in biological structures: formation of parallel bundles of actin filaments in a crystalline-like structure caused by osmotic stress. *Biochemistry* 28, 6513–6518.
- Suzuki, N., Tamura, I., Mihashi, K., 1996. Compressibility and specific volume of actin decrease upon G to F transformation. *Biochim. Biophys. Acta* 1292, 265–272.
- Ueda, T., Nakagaki, T., Yamada, T., 1990. Dynamic organization of ATP and birifrangent fibrils during free locomotion and galvanotaxis in the plasmodium of *Physarum polycephalum*. *J. Cell Biol.* 110, 1097–1102.
- Wittmann, T., Gary, M., Bokoch, G.M., Waterman-Storer, C.M., 2003. Regulation of leading edge microtubule and actin dynamics downstream of Rac1. *J. Cell Biol.* 161, 845–851.